2008

Improvement of Jc and Hc2 in MgB2 superconductor with citric acid addition

Rong Zeng
University of Wollongong, rzeng@uow.edu.au

Lin Lu
University of Wollongong, ll972@uowmail.edu.au

Jianli Wang
University of Wollongong, jianli@uow.edu.au

Wenxian Li
University of Wollongong, wenxian@uow.edu.au

Dongqi Shi
University of Wollongong, dongqi@uow.edu.au

See next page for additional authors

Journal of Physics: Conference Series **97** (2008) 012215 doi:10.1088/1742-6596/97/1/012215

Improvement of J_c and H_{c2} in MgB_2 superconductor with citric acid addition

R. Zeng*, L. Lu, J L Wang, W. X. Li, D.Q. Shi, J. Horvat and S.X. Dou

Institute for Superconducting and Electronic Materials, University of Wollongong, NSW 2522, Australia

Abstract This paper reports on the fabrication and characterization of citric acid (CA)-$C_6H_8O_7$ added MgB_2 superconductor. The relationships between microstructures, critical current density (J_c), critical temperature (T_c), upper critical field (H_{c2}), irreversibility field (H_{irr}), and normal state resistivity for 10 wt% $C_6H_8O_7$ added MgB_2 samples sintered at temperatures from 650°C to 950 °C were systematically studied. A reduction in T_c and in lattice parameter a due to the C substitution and possible oxygen (O) effects occurs with $C_6H_8O_7$ addition. J_c, H_{c2}, and H_{irr} are significantly enhanced, however, with the addition of $C_6H_8O_7$. All the samples exhibit J_c above 10^4 A/cm^2 at 5 K and 8 T. This value is higher than for the un-doped MgB_2 by a factor of 9. The significant improvement in the superconducting properties is attributed to the lattice distortion due to the C and possible oxygen (O) substitution for boron, with the C and O coming from the decomposition of $C_6H_8O_7$.

1. Introduction

MgB_2 superconductor is a promising candidate for large-scale applications at around 20 K due to its high critical temperature *(T_c)* ~ 39 K [1], as well as its cheap raw materials and simple manufacturing processing. It has been reported that a significant improvement in the critical current density (J_c) in MgB_2 can be achieved through chemical doping with nano-SiC, nano-C, carbon nanotubes (CNT), etc. [2-5], because these nanomaterials can reduce the reaction energy and decrease the reaction temperature. The C can enter the MgB_2 lattice by occupying boron (B) sites, and thus J_c and H_{c2} are significantly enhanced due to the increased impurity scattering in the two-band MgB_2. However, such nanomaterial doping processes in MgB_2 superconductor are limited by the difficulty in dispersing nanosized particles and by the poor reactivity between B and C, which will lead to inhomogeneity and increase the proportion of impurity phases, thus degrading the superconducting properties. Mickelson *et al.* first discovered B_4C as a C source [6], and Ribeiro *et al.* [5] also reported that B_4C has high potential as a C source, because during the decomposition of B_4C, highly active C particles are formed. However, they showed that a higher sintering temperature and longer sintering time are required. Dou *et al.* [7] reported enhanced superconducting properties of C doped MgB_2 from using SiC as a C source, with only a low temperature (~ 650 ◦C) sintering procedure required. Moreover, Dou's group has indicated that carbohydrates (CH) are good candidates to be C source materials for C doping into MgB_2 [8]. They decompose at temperatures that are below the formation temperature of the MgB_2 phase itself, and hence can produce highly reactive C on the atomic scale.

In this study, we report on the fabrication and superconducting properties of C doped MgB_2 superconductor when citric acid ($C_6H_8O_7$) is used as the C source. The amount of $C_6H_8O_7$ additive was

kept constant at 10 wt%, and the effects of sintering temperature on the microstructure and the superconducting properties of $C_6H_8O_7$ doped MgB_2 were studied.

2. Experimental procedure

MgB_2 bulks with addition of $C_6H_8O_7$ were prepared by an in situ reaction process. 10wt% $C_6H_8O_7$ (Aldrich, 99%) of total MgB_2 was mixed with an appropriate amount of B (99%) in toluene (99.5%). This slurry was dried in a vacuum so that the B powder was encapsulated by or mixed with the C coming from $C_6H_8O_7$. This uniform composite was then mixed with an appropriate amount of Mg (99%) powder. These mixed powders were ground, pressed, and then sintered at 650 °C to 950°C for 30 min under high purity argon (Ar) gas. The heating rate was 5°C min^{-1} under Ar. All samples were characterized by X-ray diffraction (XRD) and analyzed using Rietveld refinement XRD to determine the *a* and *c* lattice parameters and the MgO content. T_c was defined as the onset temperature at which diamagnetic properties were observed. The magnetization of samples was measured at 5 and 20 K using a Quantum Design Physical Properties Measurement System (PPMS) with a magnetic field sweep rate of 50 Oe /s and amplitude up to 9 T. The magnetic J_c was calculated from the height of the magnetization loop M using the critical state model: J_c =12Mb/d(3b-d), with b and d the dimensions of the sample perpendicular to the direction of applied magnetic field and d < b. The magnetoresistivity $\rho(H,T)$ was measured with H applied perpendicular to the current direction using the four probe method in the temperature range from 4.2 K to 300 K and the field range from 0 T to 9 T. The irreversibility field, H_{irr}, and H_{c2} can be deduced using the criteria of 0.1 and 0.9 of $\rho(H,T)$, respectively.

3. Results and discussion

Fig. 1 shows the X-ray diffraction (XRD) patterns of the doped samples sintered at 650 °C to 950 °C, as well as the un-doped sample sintered at 650°C. Analysis of the XRD patterns of the samples revealed that they are of MgB_2 phase with small amounts of MgO impurity.

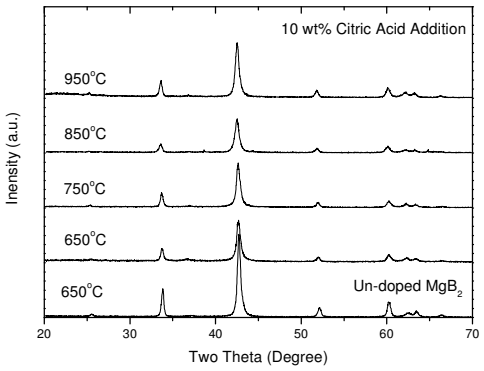

Fig. 1. X-ray diffraction patterns for the un-doped and 10 wt% citric acid added MgB_2 samples sintered at temperatures from 650 °C to 950 °C.

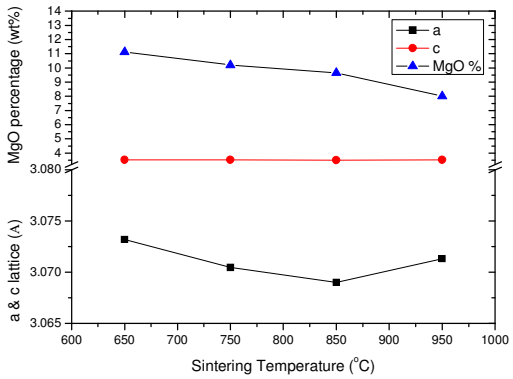

Fig. 2. The *a*- and *c*-lattice parameters and the MgO content versus sintering temperature.

Fig. 2 shows the *a*- and *c*-axis lattice parameters and the MgO content versus sintering temperature for the 10% $C_6H_8O_7$ added MgB_2 samples. It was found that both the *a*-axis and the *c*-axis lattice parameters calculated from XRD remain constant with increasing sintering temperature. From the *a*-axis data, we estimated that the amount of C substitution x was about 0.03 in the $Mg(B_{1-x}C_x)_2$ system,

according Li's [9] calculations for all 10% $C_6H_8O_7$ added MgB_2 samples sintered at different temperatures. It is particularly interesting to note that the MgO content decreases with increasing sintering temperatures. This feature is contrary to the characteristics of normal MgB_2 samples, where the MgO percentages show a slight increase with increasing sintering temperature, since high temperature sintering increases MgO precipitates [10]. This indicated that there was more formation of carbon monoxide (CO), which is a product of the decomposition of the citric acid, at high sintering temperature and that this CO acted as a reducing agent to prevent the formation of oxides of Mg and B.

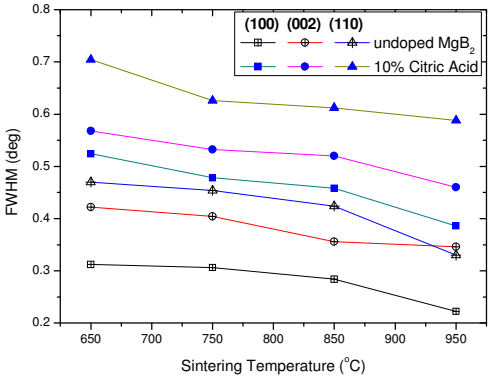

Fig. 3. Full width at half maximum (FWHM) as a function of sintering temperature for un-doped and 10 wt% citric acid added MgB_2 samples sintered at different temperatures.

The full width at half maximum (FWHM) values as function of sintering temperature for all the samples studied are shown in Fig. 3. The in-plane FWHMs of the (110) and (100) peaks for the doped samples are larger than those of the corresponding peaks for the un-doped one. As the sintering temperature increased, the in-plane FWHM values slightly decreased. Because the (110) and (100) peaks reflect the lattice constant of the honeycomb B sheet, the broadening of this peak may suggest the occurrence of some distortion of the sheet and/or some grain size refinement. This result is consistent with the report of Yamamoto et al. [12], who observed that H_{irr} increased with increasing FWHM of the (110) peak. A distortion of the honeycomb B sheet may result in an improvement in the intraband scattering, and thus enhance H_{c2} through a reduction in the coherence length ξ. A decrease in the grain size could also result in peak broadening. Typical SEM images of samples sintered at various temperatures are shown in Figure 4. It can be seen that the grain sizes of all the CA added samples are smaller than in the un-doped sample, and the grain size of the CA added sample sintered at 850 °C is slightly larger than those of the other CA added samples.

Figure 5 shows the T_c of all of the samples sintered at 650 to 950 °C for 30 min. The T_c decreased with citric acid addition, when compared to the un-doped sample, but the T_c shows slight variations with increasing sintering temperature. This could be caused by the inhomogeneity of the samples, or possibly by variations in the level of residual oxygen solubilised in the MgB_2, or in the amount of Mg evaporation, or by grain size and crystallinity variations in the samples sintered at different temperatures.

Fig. 6 shows the dependence of the J_c on the applied magnetic field (B) at 5 and 20 K. The J_c values for all of the doped samples reached 10^4 A cm^{-2} at 5 K and 8 T. These values are a factor of 6 higher than that of the un-doped MgB_2. We observed a crossover in the J_c curves at 5 K when the applied magnetic field was around 6.5 T. The crossover might be considered as an indication of the increased grain boundary pinning strength in the samples with smaller grain size and possibly of different levels of dissolved oxygen in MgB_2 samples sintered at different temperatures. For example, the lower field J_c of the 850 °C sintered sample was higher, and the high field J_c was lower than that of the others.

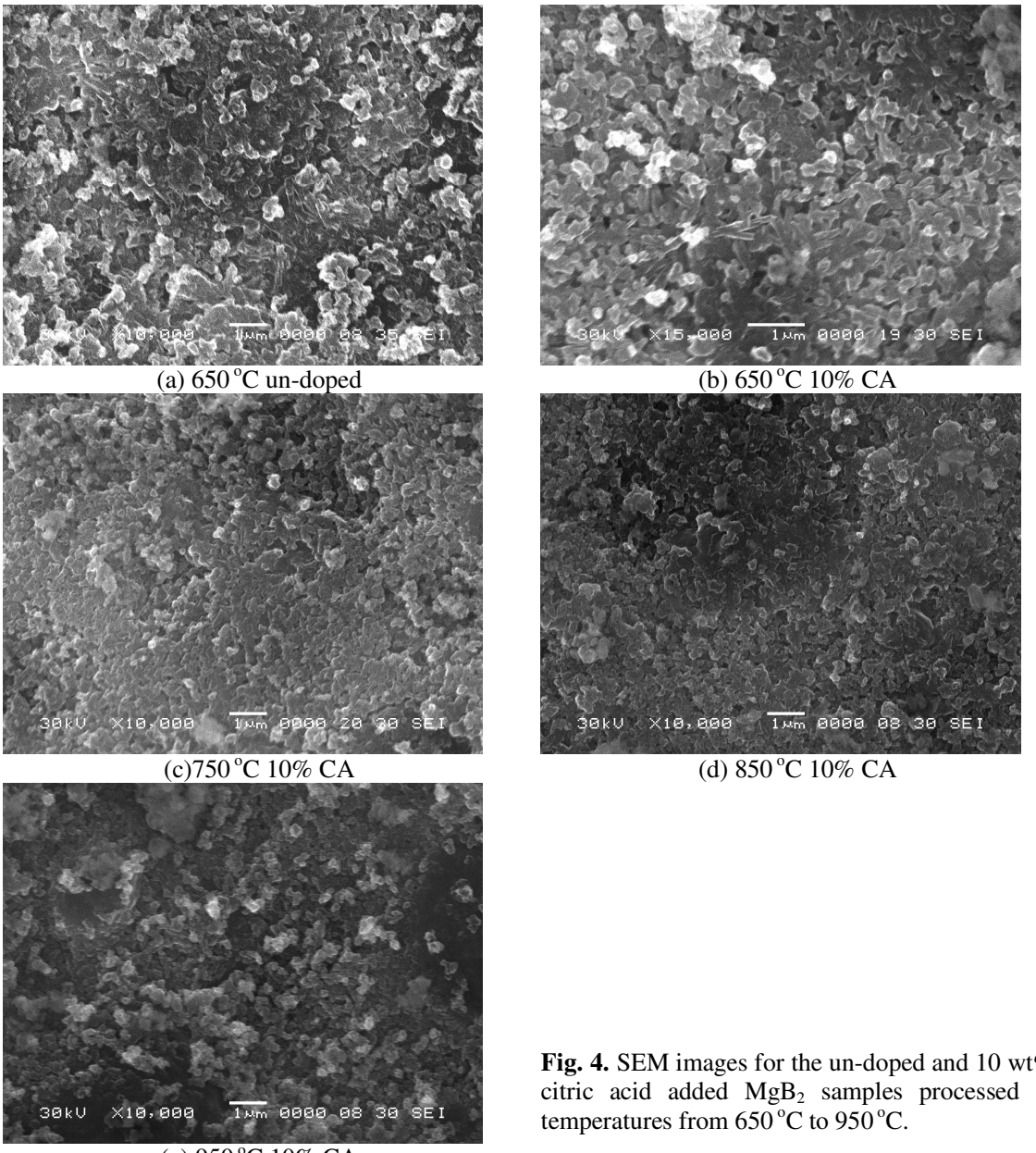

(a) 650 °C un-doped (b) 650 °C 10% CA

(c)750 °C 10% CA (d) 850 °C 10% CA

(e) 950 °C 10% CA

Fig. 4. SEM images for the un-doped and 10 wt% citric acid added MgB_2 samples processed at temperatures from 650 °C to 950 °C.

Fig. 7 shows the temperature (T) dependence of H_{irr} and H_{c2} for all of the samples. The H_{irr} and H_{c2} properties of the $C_6H_8O_7$ added MgB_2 samples are significantly enhanced compared with the un-doped sample. This enhancement in H_{irr} and H_{c2} is a result of C substitution into B sites of the MgB_2 lattice. The H_{irr} and H_{c2} of the 10% citric acid added samples show a slight variation with sintering temperature.

Fig. 8 shows the temperature dependence of the normal state resistivity of un-doped and 10 wt% citric acid added samples sintered at 650 °C to 950 °C. The higher ρ values for the 10% citric acid added MgB_2 samples indicate that the impurity scattering is stronger, due to the C substitution into B sites. The residual resistivity ratio (RRR) values varied with sintering temperature and are listed in Fig. 8. The transport properties of the samples are mainly dependent on the C substitution level, the grain

crystallinity and connectivity, and the MgO impurity phase content. In our samples, the C substitution levels of the 10% citric acid added samples are almost the same, while the varied transport properties among the 10% citric acid added samples sintered at different temperatures are due to the variations in grain crystallinity and connectivity, and in the MgO impurity phase content, which are caused by different sintering temperatures.

$C_6H_8O_7$ in the Mg and B mixture melts at lower temperatures and decomposes at temperatures below the formation temperature of MgB_2, hence producing highly reactive and fresh C on the atomic scale, as well as an assortment of gases in the reaction environment, which reduce the speed of MgB_2 grain growth, leading to a lower C substitution temperature and smaller grain size. Moreover, the fact that the C substitution possibly takes place in the gaseous state leads to very uniform C doping in the MgB_2 matrix, hence significantly enhances the critical current density and the upper critical field. However, $C_6H_8O_7$, as a typical carbohydrate, contains a large amount of oxygen, which leads to an increase in the amount of impurity phase MgO, resulting in degradation of the transport conductivity.

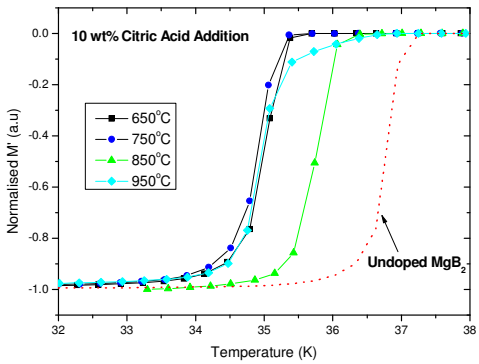

Fig. 5. The normalized ac susceptibility versus temperature (T) patterns for the un-doped and 10 wt% citric acid added MgB_2 samples sintered at different temperatures.

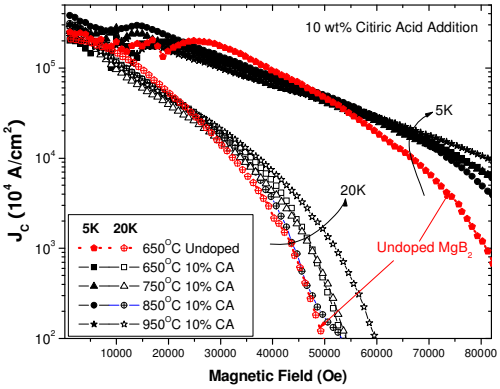

Fig. 6. The magnetic critical current density (J_c) for the un-doped and the 10 wt% citric acid added MgB_2 samples sintered at different temperatures.

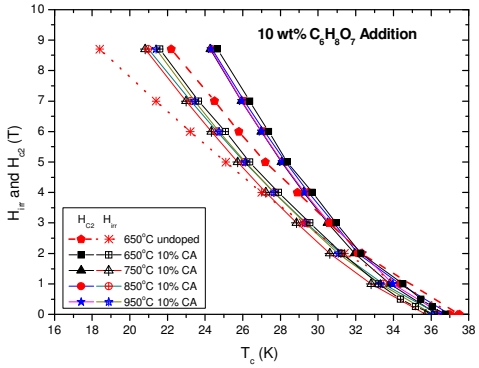

Fig. 7. Temperature dependence of the irreversibility field (H_{irr}) and upper critical field (H_{c2}) for the un-doped and 10 wt% citric acid added MgB_2 samples sintered at different temperatures.

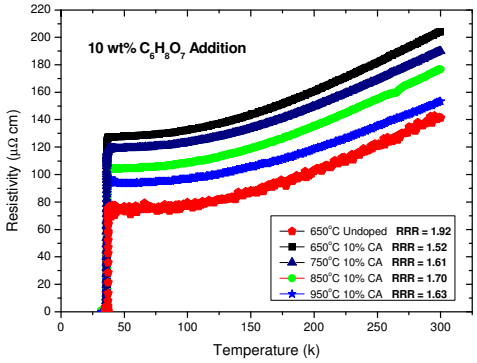

Fig. 8. Resistivity as a function of temperature from 300 down to 36 K in self-field for the un-doped and 10 wt% citric acid added MgB_2 samples sintered at different temperatures.

4. Conclusion

C-doped MgB_2 samples sintered at temperatures from 650 °C to 850 °C were prepared using 10wt% $C_6H_8O_7$ as the C source material. A decreased lattice parameter *a* in comparison with the un-doped sample indicated that about x = 0.03 of C in $Mg(B_{1-x}C_x)_2$ was substituted for B. The high field J_c values, as well as H_{irr} and H_{c2}, were significantly improved in the CA added samples, with the J_c reaching 10^4 A / cm^2 at 5 K and 8 T, which is a factor of 9 higher than for the un-doped MgB_2. These enhancements are attributed to the lattice distortion resulting from the incorporation of C atoms into the MgB_2 crystal lattice and the smaller grain size.

Acknowledgements

The authors thank Dr T. Silver and Dr J. Horvat for their help and useful discussions. This work was supported by the Australian Research Council, Hyper Tech Research, Inc., USA, and the University of Wollongong.

References

[1] Nagamatsu J, Nakagawa N, Muranaka T, Zenitani Y and Akimitsu J 2001 *Nature* 410 63.
[2] Dou S X, Soltanian S, Horvat J, Wang X L, Zhou S H, Ionescu M, Liu H K, Munroe P and Tomsic M 2002 *Appl. Phys. Lett.* 81 3419.
[3] Yamamoto A, Shimoyama J I, Ueda S, Iwayama I, Horii S and Kishio K 2005 *Supercond. Sci. Technol.* 18 1323.
[4] Yeoh W K, Kim J H, Horvat J, Xu X, Qin M J and Dou S X 2006 *Supercond. Sci. Technol.* 19 596–9.
[5] Ribeiro R A, Bud'ko S L, Petrovic C and Canfield P C 2003 *Physica* C 384 227.
[6] Mickelson W, Cumings J, Han W Q and Zettl A 2002 *Phys. Rev.* B 65 052505.
[7] Dou S X, Pan A V, Zhou S, Ionescu M, Wang X L and Munroe P R 2003 *J. Appl. Phys.* 94 1850–6.
[8] Kim J H, Zhou S, Hossain M S A, Pan A V and Dou S X 2006 *Appl. Phys.* Lett. 89 142505.
[9] Lee S, Masui T, Yamamoto A, Uchitama H, and Takama S, 2003 *Physica C* 397 7.
[10] Zeng.R, Lu L, Wang J L, Horvat J, Li W X, Shi D Q, Dou S X, Tomsic M and Rindfleisch M 2007 *Supercond. Sci. Technol*. 20 L43–L47.